

Flicker and random telegraph noise between gyrotropic and dynamic C-state of a vortex based spin torque nano oscillator

Steffen Wittrock,^{1, a)} Philippe Talatchian,^{1, b)} Miguel Romera,^{1, c)} Mafalda Jotta Garcia,¹ Marie-Claire Cyrille,² Ricardo Ferreira,³ Romain Lebrun,¹ Paolo Bortolotti,¹ Ursula Ebels,⁴ Julie Grollier,¹ and Vincent Cros^{1, d)}

¹⁾Unité Mixte de Physique CNRS, Thales, Univ. Paris-Saclay, 1 Avenue Augustin Fresnel, 91767 Palaiseau, France

²⁾Univ. Grenoble Alpes, CEA-LETI, MINATEC-Campus, 38000 Grenoble, France

³⁾International Iberian Nanotechnology Laboratory (INL), 471531 Braga, Portugal

⁴⁾Univ. Grenoble Alpes, CEA, INAC-SPINTEC, CNRS, SPINTEC, 38000 Grenoble, France

(Dated: September 8, 2021)

Vortex based spin torque nano oscillators (STVOs) can present more complex dynamics than the spin torque induced gyrotropic (G) motion of the vortex core. The respective dynamic modes and the transition between them can be controlled by experimental parameters such as the applied dc current. An interesting behavior is the stochastic transition from the G- to a dynamic C-state occurring for large current densities. Moreover, the C-state oscillations exhibit a constant active magnetic volume. We present noise measurements in the different dynamic states that allow accessing specific properties of the stochastic transition, such as the characteristic state transition frequency. Furthermore, we confirm, as theoretically predicted, an increase of flicker noise with I_{dc}^2 when the oscillation volume remains constant with the current. These results bring insight into the potential optimization of noise properties sought for many potential rf applications with spin torque oscillators. Furthermore, the investigated stochastic characteristics open up new potentialities, for instance in the emerging field of neuromorphic computing schemes.

I. INTRODUCTION

Spin torque nano oscillators (STOs) exploit magnetoresistive effects in order to convert magnetization dynamics into rf electrical signals. Exhibiting interesting properties, such as a nanometric size, complete CMOS compatibility¹, radiation hardness² and high frequency tunability³, they are considered the next-generation devices for rf applications and communications^{4,5}. However, their potentialities go even beyond this and include exploitation for hard disk reading⁶, or, based on the STOs' high responsiveness to external stimuli, broadband frequency detection⁷ and microwave energy harvesting⁸. Furthermore, along with the possibility to efficiently synchronize two or more STOs together^{9–11} in order to leverage novel neuro-inspired computing architectures for e.g. pattern recognition¹², also more complex phenomena have been demonstrated in STOs, such as stochastic^{13,14} or even chaotic^{15,16} behavior.

It has recently been shown¹⁴ that the transition between two precession modes in a vortex based STO (STVO) exhibits stochastic characteristics that can be controlled by the external parameter, i.e. the dc current or applied magnetic field. The two involved modes are the vortex core gyrotropic state and beyond, the dynamic C-state motion of the magnetization distribution with particularly interesting characteristics, such as a nearly constant magnetic oscillation volume¹⁴.

So far, the main limitation of all the above mentioned possible STO applications is their large noise characteristics, which

is necessary to be reduced and better understood. Flicker noise, that is dominant at longer timescales of sought stability, has been studied and classified mainly in the gyrotropic regime^{17,18} of a STVO. We recently found in particular a dependence of the noise level on the active magnetic volume V of the oscillation, along with the nonlinear dynamical parameters¹⁷, and predict a Hooge-like increase¹⁹ with I_{dc}^2 when the volume V is constant. In this general sense, the described C-state oscillations with constant oscillation volume V represent an interesting case to study the system's flicker noise level. Furthermore, along with the characterization of the flicker noise in the C-state, we here perform noise measurements in the transition between gyrotropic and C-state. Typical for a two-level stochastic system, we demonstrate the occurrence of random telegraph noise (RTN) within the transition, which turns out to be useful in order to better characterize the stochastic transition.

II. EXPERIMENT

The studied samples are the same as those used in Ref.¹⁴, i.e. circularly shaped nanopillars of 300nm diameter consisting of a synthetic antiferromagnetic stack (SAF) as a pinning layer. In order to exploit the tunnel magnetoresistive (TMR) effect, a MgO tunnel barrier separates the SAF and a 7nm NiFe free layer in the magnetic vortex configuration. The TMR ratio lies around 50% at room temperature and the complete layer stack is SAF/MgO(1)/Co₄₀Fe₄₀B₂₀(1.5)/Ta(0.2)/Ni₈₀Fe₂₀(7)/Ta(5)/Ru(7) with the SAF composed of PtMn(20)/Co₇₀Fe₃₀(2)/Ru(0.85)/Co₄₀Fe₄₀B₂₀(2.2)/Co₇₀Fe₃₀(0.5) and the layer thicknesses in brackets. The TMR effect converts the spin torque driven vortex dynamics into a rf electrical signal which is simultaneously measured on a spectrum analyzer and an oscil-

^{a)}steffen.wittrock@cnrs-thales.fr

^{b)}Present address: Institute for Research in Electronics and Applied Physics, Univ. of Maryland, College Park, 20899-6202, MD, USA

^{c)}Present address: GFMC, Departamento de Física de Materiales, Universidad Complutense de Madrid, 28040 Madrid, Spain

^{d)}vincent.cros@cnrs-thales.fr

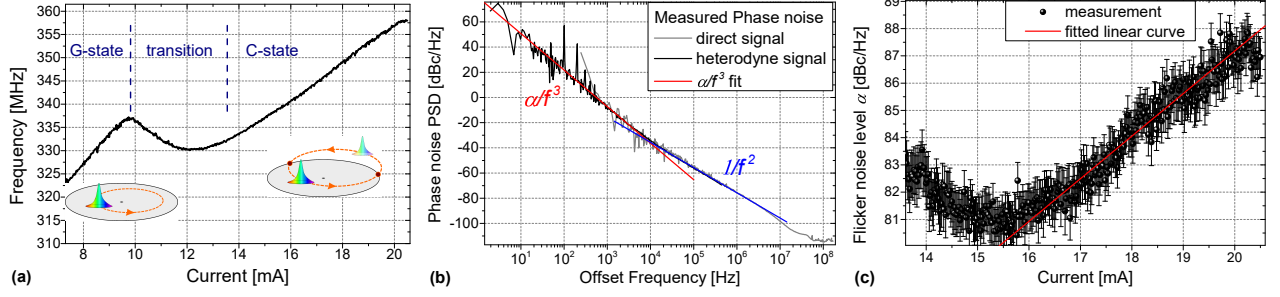


Figure 1: (a) Measured frequency vs. current evolution of the described G- and C-state regime with sketched motion of the vortex core inside/outside the nanodisk characterizing G- and C-state. (b) Phase noise curve in the C-state at 17 mA with fitted α/f^3 flicker noise contribution. (c) Corresponding flicker noise level α vs. dc current in the C-state regime. The applied perpendicular-to-plane magnetic field is $\mu_0 H_{\perp} = 520$ mT.

loscope. A perpendicular-to-plane magnetic field $\mu_0 H_{\perp}$ tilts the magnetization of the SAF's top layer in order to create a perpendicular-to-plane spin polarization providing the necessary spin torque component to reach self-sustained dynamics²⁰.

Noise data are gathered from single-shot oscilloscope voltage time traces and processing via the Hilbert transform method^{17,21,22}. To obtain noise data at low offset frequencies close to the carrier and furthermore resolve small frequency variations, a heterodyne detection technique^{17,23,24} (signal down-conversion via high-side injection and low-pass filtering (bandwidth DC to 22 MHz)) is used.

III. FLICKER NOISE IN THE C-STATE

The dynamic C-state describes the motion of the magnetic vortex core in a circular disk beyond the gyrotropic (G) state. At one point in the periodic trajectory, the vortex core reaches the disk boundary, disappears and an in-plane magnetic C-state distribution forms and precesses for a part of the oscillation period. We have recently shown¹⁴ that this behavior is mainly triggered by the presence of a field-like torque and can be identified by a rather abrupt decrease of the oscillation frequency at larger applied dc currents I_{dc} . In fig. 1, a characteristic measurement with a perpendicular-to-plane magnetic field $\mu_0 H_{\perp} = 520$ mT is shown: Recognized from the frequency vs. current curve (fig. 1a), the STVO at smaller dc currents oscillates in the G-state up to a transition from G- to C-state which stabilizes above ~ 14 mA. In fig. 1a's inset, a sketch of the vortex core trajectories is presented.

In fig. 1b, we show a phase noise measurement^{17,21,22} in the C-state, recorded at room temperature at $I_{dc} = 17$ mA. At higher frequency offsets, a $1/f^2$ noise characteristics due to thermal fluctuations is observed²⁵ while at lower frequency offsets a $1/f^3$ flicker noise process is detected¹⁷. Performing α/f^3 flicker noise fits, we present in fig. 1c the evolution of the flicker noise level α as a function of the applied dc current I_{dc} . A flicker noise minimum is reached at $I_{dc} \approx 15.5$ mA, where we assume the C-state to be stabilized after the tran-

sition. For larger applied currents, the noise level indeed increases. Performing a linear fit on the curve as depicted in fig. 1c, we find a curve slope of $\sim (1.6 \pm 0.1)$ dBc/(Hz·mA). The Hooge formula^{19,26} $\alpha \sim \alpha_H I_{dc}^2 / V$ predicts a value of 2 (note the logarithmic scale) at constant active volume¹⁷. The fact that we do not find an increase with slope of 2 but slightly lower might be explained by the complex current dependence of the Hooge-parameter α_H , a sort of quality factor of the system¹⁹, which usually decreases for higher applied bias^{17,27–29} linked to the simultaneously decreasing TMR value. Furthermore, the dynamical parameters of the oscillation, such as the damping rate back to the limit cycle, might play a role^{17,30}. In general, in the gyrotropic state the flicker noise level is decreasing with increasing current I_{dc} ¹⁷. Our measurement confirms that once the oscillation volume saturates, what is the case also in the G-state at high currents, the flicker noise level evolution however turns and increases with increasing I_{dc} , hence the Hooge formula description dominates the evolution. Thus, it means that there is a minimum in the noise level which can be exploited in order to minimize the noise level in the STO operation.

IV. RANDOM TELEGRAPH NOISE IN THE STATE TRANSITION

In fig. 2a, we show the frequency vs. current evolution of a (different) measurement at $\mu_0 H_{\perp} = 425$ mT showing a transition from G- to C-state from ~ 9 mA on. With similar characteristics of G- and C-state as before, the frequency decrease in comparison seems rather abrupt. However, traces from both of the two states are detected in the entire range from 8.9 mA up to 12.5 mA. At ~ 9.3 mA, inside the transition regime, the G-state oscillation is even stable at least for the duration of the measurement (~ 10 ms). However, within the transition the system is constantly changing between the two states with frequency differences of typically a few MHz. This is represented in the heterodyne voltage signal in fig. 2a's inset with the local oscillator frequency chosen such that it is ~ 2 MHz larger than the determined principal frequency shown in fig.

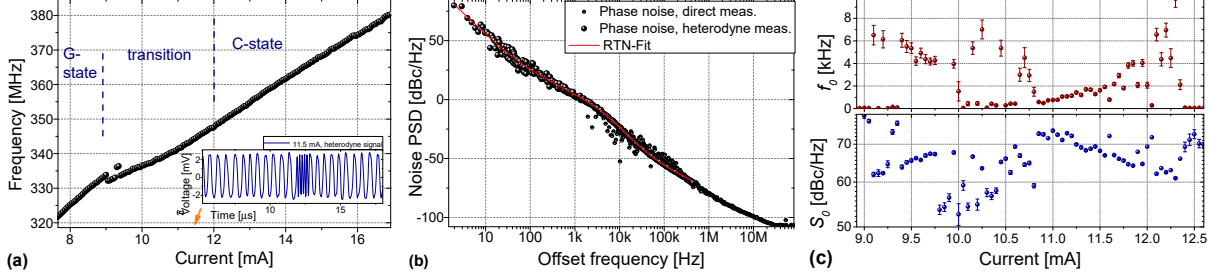


Figure 2: (a) Via spectrum analyzer measured frequency vs. I_{dc} with stochastic G→C-state transition. The inset shows a corresponding time trace of the heterodyne signal at $I_{dc} = 11.5$ mA highlighting the temporal change of state frequency, here in the interval $\sim [11.8; 12.8]$ μ s. The frequency difference of this interval to the rest of the shown curve is about 8 MHz. (b) Noise PSD with RTN fit on the phase noise data at $I_{dc} = 11.8$ mA. (c) Parameters of the RTN fits as a function of the current. The applied perpendicular-to-plane magnetic field is $\mu_0 H_{\perp} = 425$ mT.

2a. At ~ 11.8 μ s, the oscillator changes from 343 MHz into another state of 8 MHz higher frequency for a couple of periods. By performing phase noise measurements inside the transition (fig. 2b), we observe a noise PSD which is no more solely described by only thermal and flicker contributions. Instead, an additional random telegraph noise (RTN) process with a typical characteristic offset frequency f_0 of a few kHz adds to the noise PSD in fig. 2b. The appearance of such RTN contribution to the noise is found in a large range of I_{dc} from ~ 8.9 mA to ~ 12.5 mA and corresponds to the bistability of the two states, i.e. a change of frequency as also presented in fig. 2a's inset. This type of noise arises from fluctuations between two states²⁶. In order to obtain characteristic parameters of the two level time signal, we perform fits to the noise data according to²⁸

$$S_{\delta\phi} = 10 \cdot \log \left(\frac{\alpha}{f^{\beta}} + \frac{S_0}{(1 + (f/f_0)^2) f^2} \right),$$

as represented in fig. 2b. Here, α/f^{β} with $\beta \approx 3$ reflects the flicker noise at low offset frequencies. The second term describes the RTN contribution with S_0 the RTN amplitude and f_0 the characteristic RTN frequency, both chosen as fitting parameters.

The obtained RTN parameters as a function of the applied current are shown in fig. 2c. The characteristic frequency f_0 reveals that the stochastic state switching events occur on a kHz scale. It firstly decreases with increasing I_{dc} for $I_{dc} \lesssim 10.5$ mA and subsequently increases in the range $[10.6; 12.5]$ mA until the C-state oscillation becomes stable for $I \gtrsim 12.5$ mA. Note that in the range $[10; 10.6]$ mA, the characteristic frequency is partly too low for a proper parameter determination and furthermore, the frequency of the local oscillator might be between the states' frequency levels making them difficult to distinguish. Along with the probability to be in the G- or C-state, also the switching speed represented by f_0 can therefore be manipulated by the applied current, additionally adding a further system handling. In fig. 3, we analyze the state probability inside the transition more in detail. By performing Wigner-ville time-frequency spectra³¹ of the het-

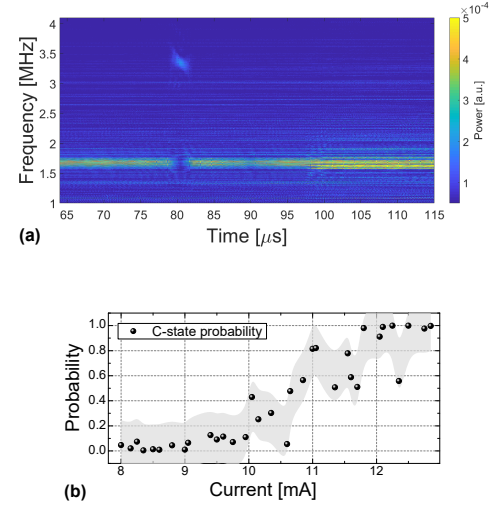


Figure 3: (a) Wigner-Ville time-frequency spectrogram at $I_{dc} = 10.25$ mA. (b) Determined C-state probability vs. current through the G- to C-state transition regime from ~ 8.9 mA to ~ 12.5 mA. Data correspond to those shown in fig. 2.

erodyne signal, such as shown in fig. 3a for $I_{dc} = 10.25$ mA, the frequency and hence the state probability can be analyzed. In fig. 3a, it is clearly seen that at ~ 80 μ s, the oscillation frequency jumps from ~ 1.7 MHz to ~ 3.5 MHz corresponding to a state change from G- to C-state. With the local oscillator at 339.3 MHz, the related real frequencies at $I_{dc} = 10.25$ mA can consequently be identified as 341 MHz for the predominant G-state and 335.8 MHz for the C-state. Note that these frequency differences are not properly resolved in the frequency determination by a spectrum analyzer as shown in fig. 2a (typical measurement duration ~ 10 ms). The probability to be in the C-state can now be analyzed and is shown in fig. 3b through the transition range. Its evolution describes a classical stochastic phase transition with the dc current as control

parameter. We recognize that a 50% probability is reached at ~ 10.6 mA, the current value where also the slope of the characteristic RTN frequency evolution is roughly estimated to invert (see fig. 2c, disregarding points with large errors between 10 and 10.6 mA). In general, random telegraph noise is a major limitation especially for magnetic sensor applications^{28,32} and can be removed here by stabilization of the G- or C-mode. However, in the sense of the G- to C-state transition, it can serve as a sort of easily accessible indicator of the probabilistic properties.

V. DISCUSSION & CONCLUSION

We present here measurements of the dynamic C-state in vortex based spin torque nano oscillators and analyze the system's phase noise characteristics. Regarding the evolution of the system's flicker noise, we find its increase with increasing applied dc current in the measured C-state regime that is dominated by Hooge's law. The measurement confirms that a minimum in the flicker noise level exists also in the G-state when the active oscillation volume saturates with the current.

At the transition between G- and C-state, we demonstrate the system oscillating for several periods in the G- and several periods in the C-state, stochastically switching between both states at a characteristic frequency in the kHz range. The occurrence of random telegraph noise in the stochastic regime is demonstrated. Its determined characteristic parameters are compared with the state probability evaluated from a time-frequency analysis and can serve as a sort of indicator of the stochasticity. The parameters show a controllable dependence of the probabilistic properties with the applied current.

We believe, firstly, that the presented results bring more insight into the noise characteristics of spin torque nano oscillators, specifically those based on the texture of a magnetic vortex, but also partly generalizable to other types of STOs. Secondly, the characterization of the stochastic transition between the two dynamic states in vortex based spin torque oscillators is an important step in order to add another feature to the exploitation of STVOs, namely stochasticity, demonstrating the STVO's capability of real multifunctionality sought in multiple technologies, such as neuromorphic systems.

ACKNOWLEDGMENTS

Gilles Cibiel, Serge Galliou and Enrico Rubiola are acknowledged for fruitful discussions. S.W. acknowledges funding from Labex FIRST-TF under contract number ANR-10-LABX-48-01. The work is supported by the French ANR project "SPINNET" ANR-18-CE24-0012. P.T. acknowledges support under the Cooperative Research Agreement Award No. 70NANB14H209, through the University of Maryland. M.R. acknowledges support from Spanish MICINN (PGC2018-099422-A-I00) and Comunidad de Madrid (Atracción de Talento Grant No. 2018-T1/IND-11935).

DATA AVAILABILITY STATEMENT

The data that support the findings of this study are available from the corresponding author upon reasonable request.

REFERENCES

- ¹A. Makarov, T. Windbacher, V. Sverdlov, and S. Selberherr, "CMOS-compatible spintronic devices: a review," *Semiconductor Science and Technology* **31**, 113006 (2016).
- ²H. Hughes, K. Bussmann, P. J. McMarr, S.-F. Cheng, R. Shull, A. P. Chen, S. Schafer, T. Mewes, A. Ong, E. Chen, M. H. Mendenhall, and R. A. Reed, "Radiation studies of spin-transfer torque materials and devices," *IEEE Transactions on Nuclear Science* **59**, 3027–3033 (2012).
- ³R. Arun, R. Gopal, V. K. Chandrasekar, and M. Lakshmanan, "Frequency enhancement and power tunability in tilted polarizer spin-torque nano-oscillator," *Journal of Applied Physics* **127**, 153903 (2020).
- ⁴N. Locatelli, V. Cros, and J. Grollier, "Spin-torque building blocks," *Nature Materials* **13**, 11–20 (2013).
- ⁵U. Ebels, J. Hem, A. Purbawati, A. R. Calafora, C. Murapaka, L. Vila, K. J. Merazzo, E. Jimenez, M.-C. Cyrille, R. Ferreira, M. Kreissig, R. Ma, F. Ellinger, R. Lebrun, S. Witrock, V. Cros, and P. Bortolotti, "Spintronic based RF components," in *2017 Joint Conference of the European Frequency and Time Forum and IEEE International Frequency Control Symposium (EFTF/IFC)* (IEEE, 2017).
- ⁶R. Sato, K. Kudo, T. Nagasawa, H. Suto, and K. Mizushima, "Simulations and experiments toward high-data-transfer-rate readers composed of a spin-torque oscillator," *IEEE Transactions on Magnetics* **48**, 1758–1764 (2012).
- ⁷A. Litvinenko, V. Iurchuk, P. Sethi, S. Louis, V. Tyberkevych, J. Li, A. Jenkins, R. Ferreira, B. Dieny, A. Slavin, and U. Ebels, "Ultrafast sweep-tuned spectrum analyzer with temporal resolution based on a spin-torque nano-oscillator," *Nano Letters* **20**, 6104–6111 (2020).
- ⁸B. Fang, M. Carpentieri, S. Louis, V. Tiberkevich, A. Slavin, I. N. Krivorotov, R. Tomasello, A. Giordano, H. Jiang, J. Cai, Y. Fan, Z. Zhang, B. Zhang, J. A. Katine, K. L. Wang, P. K. Amiri, G. Finocchio, and Z. Zeng, "Experimental demonstration of spintronic broadband microwave detectors and their capability for powering nanodevices," *Physical Review Applied* **11** (2019), 10.1103/physrevapplied.11.014022.
- ⁹S. Kaka, M. R. Pufall, W. H. Rippard, T. J. Silva, S. E. Russek, and J. A. Katine, "Mutual phase-locking of microwave spin torque nano-oscillators," *Nature* **437**, 389–392 (2005).
- ¹⁰R. Lebrun, S. Tsunegi, P. Bortolotti, H. Kubota, A. S. Jenkins, M. Romera, K. Yakushiji, A. Fukushima, J. Grollier, S. Yuasa, and V. Cros, "Mutual synchronization of spin torque nano-oscillators through a long-range and tunable electrical coupling scheme," *Nature Communications* **8** (2017), 10.1038/ncomms15825.
- ¹¹S. Tsunegi, T. Taniguchi, R. Lebrun, K. Yakushiji, V. Cros, J. Grollier, A. Fukushima, S. Yuasa, and H. Kubota, "Scaling up electrically synchronized spin torque oscillator networks," *Scientific Reports* **8** (2018), 10.1038/s41598-018-31769-9.
- ¹²M. Romera, P. Talatchian, S. Tsunegi, F. Abreu Araujo, V. Cros, P. Bortolotti, J. Trastoy, K. Yakushiji, A. Fukushima, H. Kubota, S. Yuasa, M. Ernault, D. Vodenicarevic, T. Hirtzlin, N. Locatelli, D. Querlioz, and J. Grollier, "Vowel recognition with four coupled spin-torque nano-oscillators," *Nature* (2018), 10.1038/s41586-018-0632-y.
- ¹³A. S. Jenkins, L. S. E. Alvarez, P. P. Freitas, and R. Ferreira, "Nanoscale true random bit generator based on magnetic state transitions in magnetic tunnel junctions," *Scientific Reports* **9** (2019), 10.1038/s41598-019-52236-z.
- ¹⁴S. Witrock, P. Talatchian, M. Romera, S. Menshaw, M. J. Garcia, M.-C. Cyrille, R. Ferreira, R. Lebrun, P. Bortolotti, U. Ebels, J. Grollier, and V. Cros, "Beyond the gyrotropic motion: Dynamic c-state in vortex spin torque oscillators," *Applied Physics Letters* **118**, 012404 (2021), <https://aip.scitation.org/doi/pdf/10.1063/5.0029083>.
- ¹⁵S. Petit-Watelot, J.-V. Kim, A. Ruotolo, R. M. Otxoa, K. Bouzehouane, J. Grollier, A. Vansteenkiste, B. V. de Wiele, V. Cros, and T. Devolder,

- “Commensurability and chaos in magnetic vortex oscillations,” *Nature Physics* **8**, 682–687 (2012).
- ¹⁶T. Devolder, D. Rontani, S. Petit-Watelot, K. Bouzehouane, S. Andrieu, J. Létang, M.-W. Yoo, J.-P. Adam, C. Chappert, S. Girod, V. Cros, M. Sciamanna, and J.-V. Kim, “Chaos in magnetic nanocontact vortex oscillators,” *Physical Review Letters* **123** (2019), 10.1103/physrevlett.123.147701.
 - ¹⁷S. Wittrock, S. Tsunegi, K. Yakushiji, A. Fukushima, H. Kubota, P. Bortolotti, U. Ebels, S. Yuasa, G. Cibieli, S. Galliou, E. Rubiola, and V. Cros, “Low offset frequency $1/f$ flicker noise in spin-torque vortex oscillators,” *Physical Review B* **99** (2019), 10.1103/physrevb.99.235135.
 - ¹⁸S. Wittrock, P. Talatchian, S. Tsunegi, D. Cr   , K. Yakushiji, P. Bortolotti, U. Ebels, A. Fukushima, H. Kubota, S. Yuasa, J. Grollier, G. Cibieli, S. Galliou, E. Rubiola, and V. Cros, “Influence of flicker noise and nonlinearity on the frequency spectrum of spin torque nano-oscillators,” *Scientific Reports* **10** (2020), 10.1038/s41598-020-70076-0.
 - ¹⁹F. Hooge and A. Hoppenbrouwers, “ $1/f$ noise in continuous thin gold films,” *Physica* **45**, 386–392 (1969).
 - ²⁰A. Dussaux, A. V. Khvalkovskiy, P. Bortolotti, J. Grollier, V. Cros, and A. Fert, “Field dependence of spin-transfer-induced vortex dynamics in the nonlinear regime,” *Physical Review B* **86** (2012), 10.1103/physrevb.86.014402.
 - ²¹L. Bianchini, S. Cornelissen, J.-V. Kim, T. Devolder, W. van Roy, L. Lagae, and C. Chappert, “Direct experimental measurement of phase-amplitude coupling in spin torque oscillators,” *Applied Physics Letters* **97**, 032502 (2010), <http://dx.doi.org/10.1063/1.3467043>.
 - ²²M. Quinsat, D. Gusakova, J. F. Sierra, J. P. Michel, D. Houssameddine, B. Delaet, M.-C. Cyrille, U. Ebels, B. Dieny, L. D. Buda-Prejbeanu, J. A. Katine, D. Mauri, A. Zeltser, M. Prigent, J.-C. Nalatambay, and R. Sommet, “Amplitude and phase noise of magnetic tunnel junction oscillators,” *Applied Physics Letters* **97**, 182507 (2010), <http://dx.doi.org/10.1063/1.3506901>.
 - ²³M. W. Keller, M. R. Pufall, W. H. Rippard, and T. J. Silva, “Nonwhite frequency noise in spin torque oscillators and its effect on spectral linewidth,” *Physical Review B* **82** (2010), 10.1103/physrevb.82.054416.
 - ²⁴A. Eklund, S. Bonetti, S. R. Sani, S. M. Mohseni, J. Persson, S. Chung, S. A. H. Banuazizi, E. Iacocca, M.   stling, J.   kerman, and B. G. Malm, “Dependence of the colored frequency noise in spin torque oscillators on current and magnetic field,” *Applied Physics Letters* **104**, 092405 (2014).
 - ²⁵V. S. Tiberkevich, A. N. Slavin, and J.-V. Kim, “Temperature dependence of nonlinear auto-oscillator linewidths: Application to spin-torque nano-oscillators,” *Physical Review B* **78** (2008), 10.1103/physrevb.78.092401.
 - ²⁶C. Fermon and M. Pannetier-Lecoeur, “Noise in gmr and tmr sensors,” in *Giant Magnetoresistance (GMR) Sensors: From Basis to State-of-the-Art Applications*, Smart Sensors, Measurement and Instrumentation, edited by C. Reig, S. Cardoso, and S. Mukhopadhyay (Springer Berlin Heidelberg, 2013).
 - ²⁷A. Gokce, E. R. Nowak, S. H. Yang, and S. S. P. Parkin, “ $1/f$ noise in magnetic tunnel junctions with MgO tunnel barriers,” *Journal of Applied Physics* **99**, 08A906 (2006).
 - ²⁸J. M. Almeida, P. Wisniowski, and P. P. Freitas, “Low-frequency noise in mgo magnetic tunnel junctions: Hooge’s parameter dependence on bias voltage,” *IEEE Transactions on Magnetics* **44**, 2569–2572 (2008).
 - ²⁹F. G. Aliev, R. Guerrero, D. Herranz, R. Villar, F. Greullet, C. Tiusan, and M. Hehn, “Very low $1/f$ noise at room temperature in fully epitaxial fe/MgO/fe magnetic tunnel junctions,” *Applied Physics Letters* **91**, 232504 (2007).
 - ³⁰A. Slavin and V. Tiberkevich, “Nonlinear auto-oscillator theory of microwave generation by spin-polarized current,” *IEEE Transactions on Magnetics* **45**, 1875–1918 (2009).
 - ³¹L. Cohen, *Time-frequency Analysis*, Electrical engineering signal processing (Prentice Hall PTR, 1995).
 - ³²H. Weitensfelder, H. Brueckl, A. Satz, K. Pruegl, J. Zimmer, S. Lubner, W. Raberg, C. Abert, F. Bruckner, A. Bachleitner-Hofmann, R. Windl, and D. Suess, “Comparison of sensitivity and low-frequency noise contributions in giant-magnetoresistive and tunneling-magnetoresistive spin-valve sensors with a vortex-state free layer,” *Physical Review Applied* **10** (2018), 10.1103/physrevapplied.10.054056.